Field test demonstration of Adaptive Optics pre-correction for a Terabit Optical Communication Feeder Link

Broekens, K. A.; Doelman, N. J.; Klop, W. A.; Silvestri, F.; Do Amaral, G. C.; Vos, Y.; Veldhuis, E. P.; Korevaar, C. W.; Saathof, R.; More Authors

DOI
10.1109/ICSOS59710.2023.10490281

Publication date
2023

Document Version
Final published version

Published in
2023 IEEE International Conference on Space Optical Systems and Applications, ICSOS 2023

Field test demonstration of Adaptive Optics pre-correction for a Terabit Optical Communication Feeder Link

2023 IEEE International Conference on Space Optical Systems and Applications (ICSOS) | 979-8-3503-0790-0/23/$31.00 ©2023 IEEE | DOI: 10.1109/ICSOS59710.2023.10490281

K.A. Broekens[1], N.J. Doelman[1,2], W.A. Klop[1], F. Silvestri[1], G.C. do Amaral[1], Y. Vos[1], E.P. Veldhuis[1], T.-C. Bui[1], C.W. Korevaar[1], I. Ferrario[1], R. Saathof[3]

[1] TNO, Unit High-Tech Industry, [2] Leiden University, Faculty of Science, [3] Delft University of Technology, Aerospace Eng.

***Abstract* — A 10 km ground-to-ground field test of a Terabit/s Optical Feeder Link demonstrator has been carried out. The demonstrator aimed for end-to-end communication performance with the use of Adaptive Optics pre-correction to mitigate the atmospheric turbulence disturbances of the FSO channel. It further includes the multiplexing of multiple uplink channels and RF end-to-end modems to prove the technical feasibility of supporting a Terabit/s communication link. The field test - performed in July 2022 - demonstrates error free communication for over 10 minutes. This achievement proves the feasibility of a digital transparent communication architecture for the Terabit/s Feeder link application. The field test results are presented jointly with a companion paper [1] which focusses on the communication aspects. The Adaptive Optics (AO) pre-correction performance is analyzed against the atmospheric turbulence strength and the number of corrected AO modes. The encountered turbulence conditions during the field test caused irradiance fluctuations in the strong fluctuation regime. The field test results show a significant AO wavefront error correction on the downlink. For the uplink irradiance levels, a modest advantage of pre-correcting higher wavefront modes is found against the pre-correction of only the tip-tilt modes. Finally, with respect to the uplink fading characteristics, the AO pre-correction leads to a reduction of the mean-fade time of approximately 20-30%, compared to AO tip-tilt pre-correction only.**

Keywords— Optical satellite communication, adaptive optics, pre-correction, wave front sensor, deformable mirror, ground-to-ground link demonstrator, RF end-to-end transparent optical communication

I. INTRODUCTION

Achievable data rates for satellite communications based on radio frequencies (RF) will very soon reach its limits, due to the limited availability of the RF spectrum [2]. In order to overcome this limit, specifically focusing on bi-directional links between ground stations and very high throughput GEO satellites, TNO envisions optical free-space communication [3], [4], [5]. For the next generation of very high throughput communication satellites, feeder links based on free-space optical (FSO) communication offer a vast increase in data throughput over RF links. However, the FSO channel impairments caused by atmospheric turbulence are a major challenge for an optical uplink between ground and space terminals. To mitigate the distortion by atmospheric turbulence, TNO proposes a cross-layer combination of communication technology and Adaptive Optics (AO) for real-time pre-correction of the optical beam.

Within the Terabit Optical Communication Adaptive Terminal (TOmCAT*) project an Optical Ground Terminal (OGT) demonstrator is being developed by TNO for the Terabit/s optical feeder link application. The (TOmCAT) project focusses on reducing the risk in the development of an Optical Feeder Link (OFL) product. Within TOmCAT, the OGT Demonstrator is a successor to the Optics Feeder Link Adaptive Optics (OFELIA) breadboard [3], [4] and the AO demonstrator field test [6]. The OGT Demonstrator aims to verify end-to-end communication with AO pre-correction technology in a ground-to-ground field test over 10 km. This demonstration includes the multiplexing of multiple high power uplink channels and RF end-to-end modems to prove the technical feasibility of supporting a Terabit/s communication link.

Contemporary research and field tests on the performance of Adaptive Optics pre-correction for optical feeder links has been reported in [10] (FEEDELIO experiment) and [11] (Alpha Up in-orbit test).

**TOmCAT is part of the ESA ARTES Strategic Programme Line (SPL) 'Optical & Quantum Communications', also known as 'ScyLight'.*

II. OGT DEMONSTRATOR

The OGT demonstrator test campaign is the second and last field test in TOmCAT phase 2 and focusses on establishing the optical end-to-end communication link. The OGT demonstrator aims to verify the following combined technologies: AO pre-correction, RF end-to-end modems and high power optical channel multiplexing. During the test campaign three different types of tests were performed: the single-channel tests, the multi-channel tests and a DVB-S2(x) test.

The single channel communication tests consist of an active channel at a single wavelength at 1553.33 nm. The multi-channel test adds two dummy channels (1551.72 and 1554.95 nm) on top of the single channel communication, to verify the operation of the free-space high optical power Bulk Multiplexer (BMUX [7]) and also the wavelength separation at the demultiplexer. The dummy channels with random bit streams are generated by two Acacia modules (CFP2-DCO). In the third and final test the transmitter and receiver modem are included to enable the full RF end-to-end communication link.

The AO pre-correction strategy is based on a 'classic' AO post-correction system of the incoming downlink optical beam. The underlying assumption is that such a correction is also effective for the uplink optical beam to satellite. Thereby, it is assumed that the angular anisoplanatism caused by the point-ahead angle causes limited degradation of the correction performance. To investigate the impact of the

anisoplanatism, the number of AO modes of the pre-correction has been made tuneable.
The AO system of the OGT consists of a Shack Hartmann Wavefront Sensor (WFS) and two active mirrors: the Deformable Mirror and the Fine Steering Mirror. Both the downlink beam and the uplink beam pass the Deformable Mirror and Fine Steering Mirror surface, which are driven by the AO controller based on the measured wavefront phase error in the downlink beam path [3].

For the AO performance analysis, only the single and multi-channel tests are regarded. Since the multiplexer functionality was already verified in the laboratory for all channels [7] and the power measurements used in this analysis are equally sensitive for all channels used during field test, no differentiation is made between the single and multi-channel tests in the analysis performed in this paper. The cumulative transmitted EDFA power over all channels is used to normalize the received power traces. This enables the evaluation of the overall link loss.

For more details about the communication hardware layout, the DVB-S2(x) test and the achieved communication performance with single and multi-channel the reader is referred to the companion paper [1].

This OGT demonstrator is a follow-up of the AO demonstrator and therefore re-uses the hardware as presented in [6]. The hardware is upgraded to facilitate the end-to-end communication testing. In the upcoming sections the upgrade to OGT demonstrator is further detailed.

A. Optical Ground Terminal

First, the BMUX [7] has been merged with the OGT underneath the main optical breadboard. The BMUX demonstrator enables the use of up to 5 wavelengths co-aligned for the uplink. Second, the communication equipment has been integrated as described in [1], consisting of one active channel and two dummy channels for verification of the cross coupling behaviour.

The AO performance has been improved by updating the AO modes, which define the 2D spatial corrections applied by the feedback AO control algorithm. Furthermore, apart from turbulence-induced wavefront correction, the DM is regularly calibrated, such to minimize the quasi-static optical bench errors. This static DM shape calibration is referred to as the best flat (wavefront) condition. Due to thermo-mechanical drift this best flat DM shape requires regular updates, which was one of the upgrades with respect to the previous field test [6].

Figure II-1: Test bed of the OGT demonstrator (left) and the OGT demonstrator trailer during the field test (right)

B. Space Terminal Breadboard

The Space Terminal Breadboard (STB), used as counter terminal, has been upgraded to its OGT configuration to represent the receiving end of the uplink communication. The breadboard has been modified to enable the coupling into a fiber, which is relayed to a fiber-based Power Meter (PM) and the communication equipment via a fixed ratio splitter. The optical power received by the Power Meter is recorded at a 2 kHz sampling rate and is being used as measure for the optical power received by the communication branch.

The measurement scripts have been extended to interface with the additional hardware. Both OGT and STB hardware are configured and logged by an automated test script. This hierarchy ensures that the same settings are used on both sides and that the data and performance measurements of both terminals are performed synchronously.

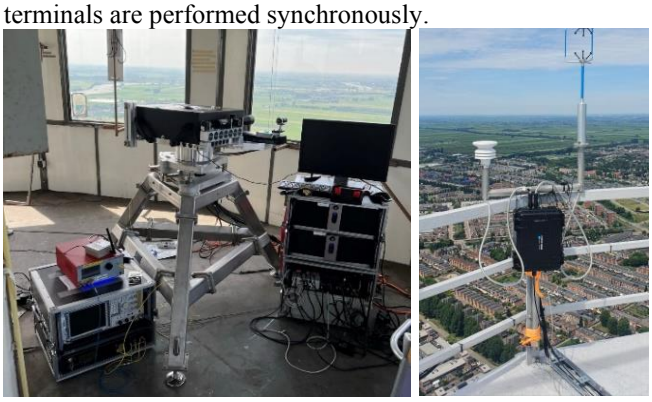

Figure II-2: STB located in the crow's nest (left) and TM4 located at the roof of the Gerbrandy tower (right)

C. Turbulence Monitors

Local turbulence effects have a major impact on the optical beam distortions and therefore monitoring of local turbulence is key during the field test. In total four Turbulence Monitors (TM's) have been placed along the slant path as schematically represented in Figure II-3. Each turbulence monitor contains a sonic wind meter (for measuring wind speed and direction) and a weather station (pressure, temperature and humidity measurements). Two TM's have been placed on the tower to avoid the impact of the tower's wake, whereby a TM is selected based on wind direction. The TM's are synchronized with a GPS timestamp to allow matching the turbulence data to the link measurements.

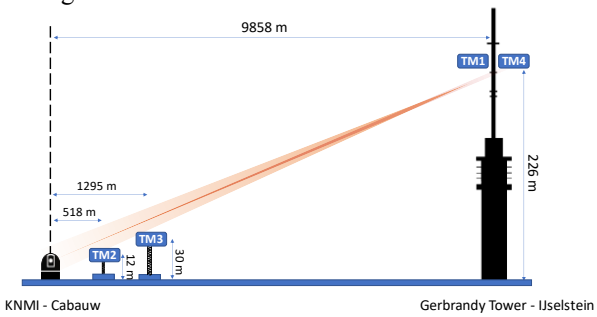

Figure II-3: Field test layout indicating the link path and position of Turbulence Monitors

III. FIELD TEST DESCRIPTION

The field test was performed over the span of 4 weeks in July 2022. The field test campaign was executed at a site as

described in [6] located southwest of the city of Utrecht, Netherlands. As depicted in Figure II-3 and Figure III-1, the link spans approximately 10 km from the OGT demonstrator trailer located in Cabauw to the STB placed at a height of 226 meters inside the Gerbrandy tower in IJsselstein. The inclination of the link was approximately 1.3°, whereby the area in between is flat and mostly covered with grassland. The measurement campaign was executed over the span of several days during daytime (10 to 7 pm CET).

Figure III-1: Field test location of the STB (left) and OGT (right)

A. Test Procedure

During the field test a series of measurement sweeps are performed to execute a sequence of measurements in a predetermined order with various system configuration parameters. For each measurement sweep a fixed Point Ahead Angle (PAA) and Wavelength Division Multiplexing (WDM) mode is chosen, while the communication mode and AO mode is being varied during the sweep. Table III-1 provides a comprehensive list of parameter values used during the field test, except for the communication mode. A total test sweep covers approximately 1 hour, whereby each configuration is measured over 30 seconds.

The number of applied AO modes is being alternated, ranging from 2 to 28 AO modes during the field test. In this context, 2 AO modes refers to the tip-tilt modes. The tip-tilt configuration primarily serves as a reference for assessing the improvement achieved by higher AO modes in relation to this tip-tilt configuration. This is referred to as (higher mode) AO gain in the remainder of this paper, which is obtained by dividing the measured irradiance with the higher AO modes by the irradiance measured during the preceding tip-tilt measurement in the sweep. An AO gain higher than unity therefore indicates an improvement with respect to the tip-tilt configuration. The configuration without AO pre-correction was not tested, as the expected losses were considered too high to establish the communication link. Therefore, minimally 2 AO modes (tip-tilt) are controlled.

Table III-1 Optical and AO system configurations

MODE	SETTING	DESCRIPTION
AO mode	2, 8, 16, 28	AO modes (pre-)correction
PAA mode	0, 18	Point-ahead angle in µrad
WDM mode	1	Single wavelength at 1553.33 nm
	3	Multiple wavelengths of 1551.72, 1553.33, 1554.95 nm

The AO configuration is swept over the various mode configurations detailed in Table III-1, whereby the PAA and WDM configuration remain fixed. The WDM mode is not expected to have impact on the link performance, therefore the distinction in WDM mode is left out of the analysis and the accumulative power of all channels is used instead. For variations of communication settings, such as FEC code rate and interleaver length, the reader is referred to the companion paper [1].

B. Meteorological conditions

The weather and turbulence conditions were measured by the TM's along the link path. These TM measurements allow for quantification of the encountered turbulence strength and are both used in the presentation of results and as input for simulation. Figure III-2 and Figure III-3 show the temperature and windspeeds recorded by the TM's during the field tests.

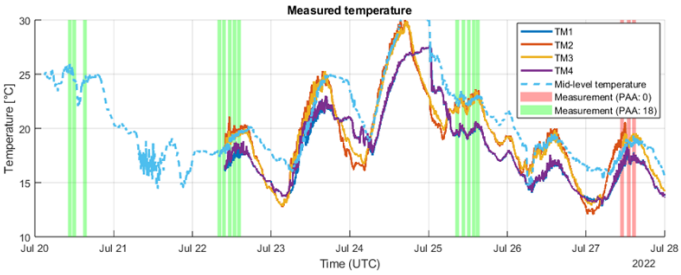

Figure III-2:Temperature measured by the turbulence monitors during the field test

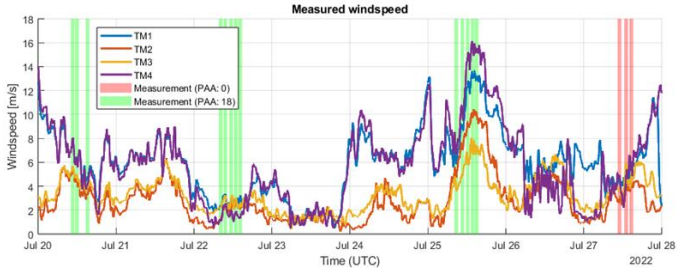

Figure III-3: Windspeed measured by TM's during the field test

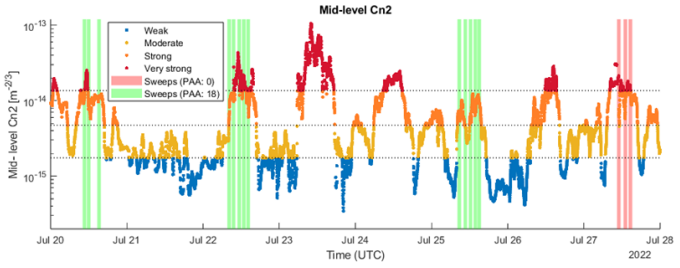

Figure III-4: Mid-level Cn2 values based on interpolated TM measurement profile

These local meteorological measurements are used as input to derive the Cn2 behavior using the method prescribed in [8]. Apart from the Cn2-profile, also the measured wind speed is used as input for the simulations. Further analysis based on simulation of the actual profile can be found in [9].

The three TM measurements are used as input to estimate the Cn2-profile encountered during the measurement based on spatial linear interpolation. This interpolated turbulence profile is used as input for the turbulence simulations.

For one of the representations of the turbulence strength the median of the interpolated turbulence profile is used, which is the expected turbulence at 113m height based on linear interpolation of TM3 and TM1/4. This mid-level Cn2 is identical to the median Cn2 used in [6].
To categorize the turbulence conditions, the measurements are binned based on the mid-level Cn2 ranges indicated by Table III-2. This categorization is performed to evaluate the average AO gain for a specific turbulence strength condition.

Table III-2: Turbulence strength categorization based on the interpolated turbulence path and number of occurrences of these conditions versus PAA setting.

TURBULENCE CATEGORY	MID-LEVEL Cn2 RANGE [$M^{-2/3}$]	RYTOV VARIANCE RANGE [-]	OCCURANCES µRAD PAA	
			0 µrad	18µrad
Weak	< 1.7 x 10^{-15}	< 2.4	0	0
Moderate	1.7 – 4.7 x 10^{-15}	2.4 – 6.7	0	54
Strong	4.7 - 13.6 x 10^{-15}	6.7 – 18.5	78	361
Very strong	> 13.6 x 10^{-15}	> 18.5	53	113

Note, that for most test days the turbulence conditions fall in the strong or very strong category. In some cases, a moderate condition has been encountered. No tests were performed under 'weak' turbulence conditions, which were only present at night-time during this period (Figure III-4).
Nevertheless the Cn2-values measured at ground level during the field test (TM2) match the order of magnitude of ground level values of commonly used HV-5/7 model.

IV. Results

A. Downlink AO Correction

First the AO performance of the downlink has been verified, particularly in terms of residual Wavefront Error (WFE). In Figure IV-1 the residual WFE measured by the Wave Front Sensor (WFS) is depicted as function of the encountered mid-level turbulence strength and the number of corrected AO-modes. The residual WFE shows an increasing trend with stronger turbulence strengths as expected. Furthermore, correcting more AO modes leads to a higher wavefront error rejection.

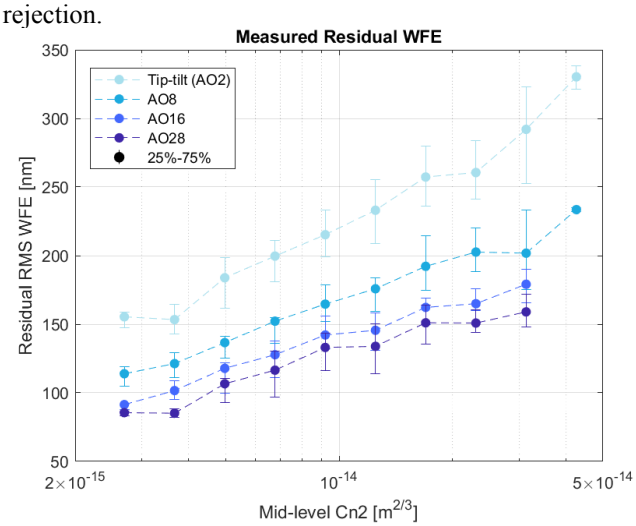

Figure IV-1: Residual RMS WFE as function of the turbulence strength for various AO mode configurations

Compared to the results described in [6] the residual WFE for a small amount of AO modes (2 and 8) is considerably lower. This is a result of the more frequently updated DM best flat shape.

The measured WFE values have been cross-checked with a simulation model. This model is based on a Kolmogorov turbulence spectrum and a Zernike mode decomposition. It includes the spatial (fitting) error and the time-delay error. Furthermore, the static systematic wavefront error of the AO bench – which contributes to the total WFE - was determined based on verification lab test at 49 nm (RMS).
Figure V-2 shows the simulated residual error against the measured error, in which the static WFE has been incorporated. Note, that the dashed line represents the case of a 100% match between simulated and measured residual errors.

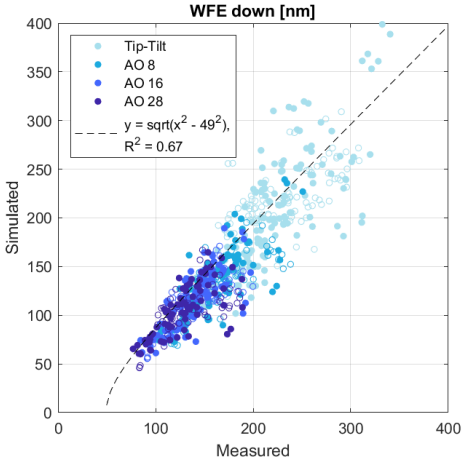

Figure IV-2: Measured versus Simulated Residual RMS WFE for various AO mode configurations

The simulation and measurement show a good correlation (R^2=0.67), which confirms that the AO has been functioning correctly. Generally, the measured residual WFE tends to be slightly higher than the simulated. The residual scattering is expected to lie in the uncertainty of the actual turbulence profile.

B. Uplink loss distributions

In the earlier analysis [6] the mean link loss encountered by the uplink as function of the turbulence strength and number of AO modes was presented for the AO demonstrator field tests. Here, we focus on the probability distribution of the link loss, which is directly related to the (normalized) received irradiance levels. This is relevant for free-space optical communication with respect to fading behavior.

The measured link loss distributions for each AO and PAA configuration are averaged per turbulence category. For each category the various AO mode configurations are analyzed for both 0 and 18 µrad PAA; see Figures IV-3 and IV-4 respectively for the 'strong' and 'very strong' turbulence categories, whereby the vertical lines represent the average irradiance levels.

In Figure IV-3 it can be observed that for the 'strong' turbulence category:

0 µrad PAA: Pre-correction of higher AO modes shows a clear decrease in link loss (~1.5 dB), compared to pre-correction of the tip-tilt mode only. Also, the fade depth is (partially) reduced by higher order AO pre-correction, as the probability in the tail of the link loss distribution is reduced.
18 µrad PAA: Pre-correction of higher AO modes shows a limited reduction in link loss, compared to pre-correction of the tip-tilt mode only. The 8 AO modes shows thereby the highest reduction. Still, differences in link loss distribution between the various AO mode cases are relatively small (<1 dB).

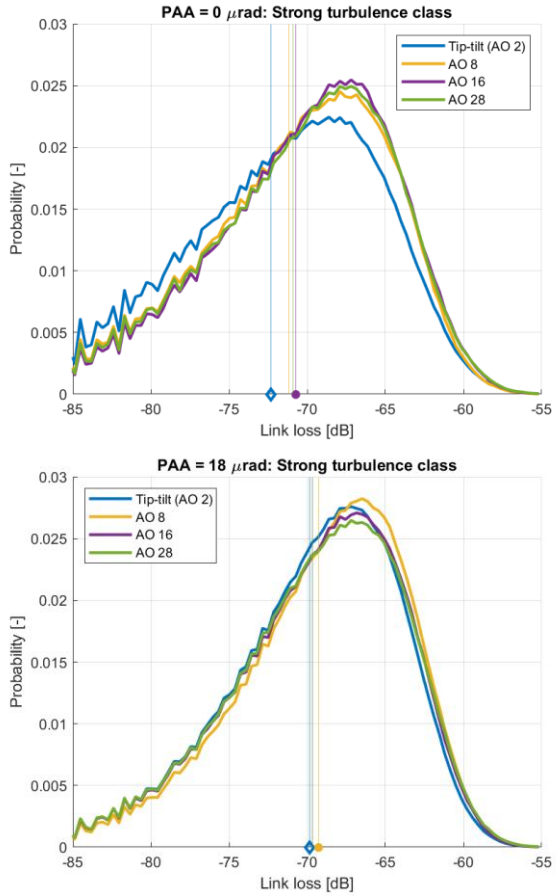

Figure IV-3: Strong turbulence condition - 0 µrad PAA (top) and 18 µrad PAA (bottom)

In Figure IV-4 it can be observed that for the 'very strong' turbulence category:
0 µrad PAA: Pre-correction of higher AO modes shows again a decrease in link loss, compared to pre-correction of Tip-tilt only. The 16 modes configuration shows the best reduction in link loss based on the average link loss profile.
18 µrad PAA: Pre-correction of higher AO modes shows a reduction in link loss, compared to pre-correction of tip-tilt only. The 8 modes configuration seems to perform slightly better based on the average link loss profile. Still, differences between the various AO mode cases are relatively small (<1 dB).
The averaged link loss profiles show that for both turbulence categories, the highest number of corrected AO modes does not yield the highest pre-correction performance. This is due to the increasing sensitivity to angular anisoplanatism with (Zernike) mode order; see also [12].

Note that the turbulence profile varies between measurement days and even over the course of a single day. This effect is not captured in a single turbulence strength metric such as the mid-level Cn2 and the accompanied turbulence categorization (Table III-2). A comparison of absolute link loss values between PAA's, measured on separate days, is therefore likely unreliable due to their expected variation in link profiles. Specifically, Figure IV-3 might suggest that the link loss for 0 µrad PAA is higher than the 18 µrad PAA configuration, which contradicts to what is expected.

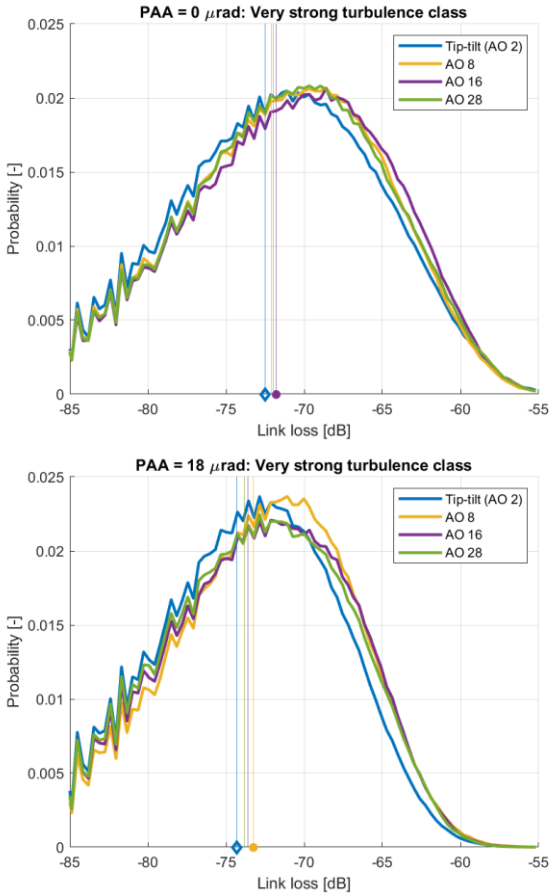

Figure IV-4: Strong turbulence condition - 0 µrad PAA (top) and 18 µrad PAA (bottom).

C. Fade Levels

An essential parameter next to the link loss distribution are the fade characteristics. If the irradiance level goes below a certain sensitivity threshold of the receiving terminal, the fading results in bit errors or in the worst case the signal is temporarily lost. The fade depth determines the required dynamic range of the optical communication terminal. For the fade depth analysis only the 18 µrad is regarded as it was considered to represent the ground-to-GEO use case. As can be observed from Table III-2, the majority of the measurements were performed in this configuration which covers a larger range of turbulence conditions.

The fade depth is determined by first normalizing the irradiance traces by their respective means. The cumulative distribution function of the normalized irradiance values is displayed for the various turbulence conditions for both 2 AO modes as well as 28 AO correction modes in Figure IV-5.

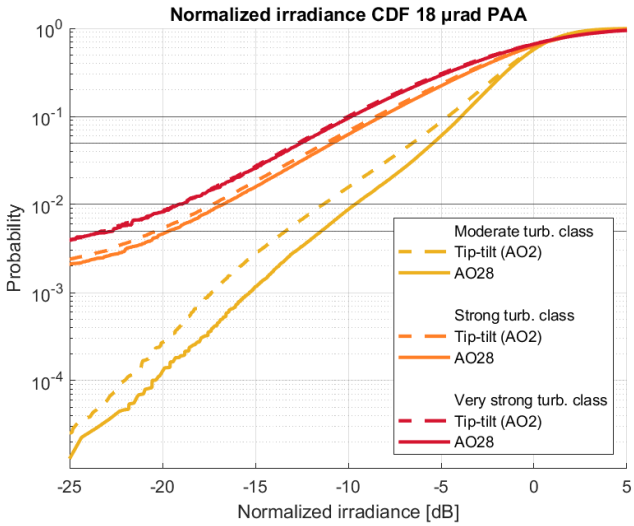

Figure IV-5: Cumulative distribution function of received irradiance at STB PM for all datasets under moderate, strong and very strong turbulence conditions, with PAA=18 µrad.

The cumulative density function shows an increasing probability of deep fade levels with increasing turbulence strengths, as expected. The advantage of 28 AO modes correction over 2 AO modes correction, ranges from ~2 dB (moderate turbulence) down to below 1 dB for very strong turbulence. Further details are given in Table IV-1, in which the fade levels are shown corresponding to various outage percentages.

Table IV-1: Fade levels for moderate and strong turbulence conditions at 18 µrad PAA.

Fade levels - Moderate turbulence case		
Outage %	Fade level [dB]	
	2 AO modes	28 AO modes
10 %	-4.63	-3.91
5 %	-6.53	-5.42
1 %	-11.36	-9.64
0.5 %	-13.36	-11.43

Fade levels - Strong turbulence case		
Outage %	Fade level [dB]	
	2 AO modes	28 AO modes
10 %	-8.50	-8.20
5 %	-11.21	-10.82
1 %	-17.33	-16.75
0.5 %	-20.35	-19.68

D. Fade Durations

Next to fade depth, the fade duration properties are also of interest for the communication performance. Free-space optical channels generally suffer from relatively long fades (order of ms), as a result of the (relatively) long correlation properties of the channel impairments. The impact of fades can be overcome by applying sufficiently long interleavers. However, the use of interleavers leads to an additional latency of the optical link. In Table IV-2 the fade duration statistics are presented for the measured cases and AO system settings.

Please note that the outage percentages for two AO configurations are relative to their respective irradiance means and relative fade levels. Therefore the fade durations correspond to different absolute irradiance threshold values.

Table IV-2: Fade duration statistics for moderate and strong turbulence conditions at 18 µrad PAA.

Fade duration – Moderate turbulence				
Outage %	Mean [ms]		STD [ms]	
	2 AO modes	28 AO modes	2 AO modes	28 AO modes
10 %	10.8	8.65	11.2	9.93
5 %	8.72	7.18	8.47	7.81
1 %	5.58	4.55	4.74	4.32
0.5 %	4.54	3.81	3.61	3.31

Fade duration – Strong turbulence				
Outage %	Mean [ms]		STD [ms]	
	2 AO modes	28 AO modes	2 AO modes	28 AO modes
10 %	6.52	4.59	6.55	4.59
5 %	4.86	3.37	4.95	3.37
1 %	2.67	1.92	3.82	1.92
0.5 %	2.17	1.56	3.99	1.56

From the tabular results shown above it follows that correcting 28 AO modes leads a significant reduction of the mean fade times, compared to correcting 2 AO modes. A similar conclusion holds for the standard deviation of the fade durations.
Also, the mean and standard deviation of the fade durations clearly decrease with increasing turbulence strength by 20-30%, which indicates that although the fades become deeper they last for a shorter period.

V. Conclusions

The OGT demonstrator field test has been performed over the span of four weeks, whereby the link performance has been measured in various AO and PAA configurations. Next to the primary test goal of an end-to-end communication link, the test allows for the evaluation of performance gain of the AO pre-correction system to enhance the overall throughput on the uplink.

The encountered turbulence conditions have been severe during the test campaign as a result of high temperatures and clear conditions especially in the middle of day. For the vast majority of the conditions the Rytov variance has been well above 1, which corresponds to the strong fluctuations regime. Apart from the strong fluctuations regime, also the extremely low elevation angle of the field slant path has made the setting much more challenging than a ground-to-GEO satellite link.

Still, the AO system performance has been verified to operate correctly even in these extreme turbulence conditions, which was given by the measured residual WFE in various AO configurations. A good correlation (R^2=0.67) between measured and simulated residual WFE has been found.

With the ground-to-GEO link in mind, the point-ahead angle has been set to 18 µrad, which is a geometrical representative for the ground-to-GEO case. The effective isoplanatic angle for the field test cases – however – turns out to be at least a factor ~10 lower than for ground-to-GEO case (with HV-5/7 model). Hence, a representative angular anisoplanatic case would have been created with a PAA <2 µrad. Therefore, the

0 µrad PAA test results presented here are expected to be more representative than the 18 µrad PAA case.

For the uplink, the gain of higher order AO over 2 AO modes correction was observed to be ~1.5 dB for 0 µrad PAA for the strong turbulence conditions. This gain reduces to 1 dB for the very strong conditions (Rytov variance > 18.5). For a point-ahead angle of 18 µrad the higher order AO gain is about 1 dB for both strong and very strong turbulence conditions.

With respect to fade behaviour, quite a significant reduction of the fade duration has been observed when correcting 28 AO modes instead of 2 AO modes. A decrease of 30% is found for the mean and the standard deviation of the fade duration.

Overall, the analysis has shown that using more than 2 AO modes in pre-correcting the uplink optical beam, leads to modest performance improvements in this field test. To a great extent, this is inherent to a field test over a 10 km near-horizontal slant path. This link configuration leads to very small isoplanatic angle values. It is therefore expected – and confirmed by numerical models – that in an actual ground-to-satellite link, the gain of higher order AO mode pre-correction will be higher. Hence, this study shows that Adaptive Optics pre-correction can increase the performance of optical feeder links by enhancing throughput, reducing error rate and by reducing latency.

ACKNOWLEDGMENT

We would like to thank J. Frijns and M. Pierzyna for their efforts in activities affiliated to the data processing of the OGT demonstrator. Our appreciation goes to N. Planjer and S.K. Mahalik in supporting the documentation. Further we hereby express our gratitude to L. Feenstra, W.J. van der Hoogt, P. Toet and M.J.J. Baeten for their help with the integration of the OGT demonstrator.

This study has been conducted as part of the Terabit Optical Communication Adaptive Terminal (TOmCAT) project (contract 4000121503/17/NL/US), which is part of ESAs ARTES Scylight program.

REFERENCES

[1] W. Korevaar et al., “Terabit Optical Feeder Links for DVB Satellite Systems: Real-time End-to-End Communication System Design & Field Test Results” in press, International Conference on Space Optical Systems 2023.

[2] H. Hemmati, Near-Earth Laser Communications. CRC Press, 2009.

[3] R. Saathof et al., “Adaptive Optics pre-correction for Optical Feeder Links – breadboard performance” in International Conference on Space Optical Systems, 2018.

[4] R. Saathof et al., “Pre-correction Adaptive Optics Performance for a 10 km Laser Link”, Spie Proc. Free-Space Laser Communications XXXI (Vol. 10910, pp. 325-331), March 2019.

[5] R. Saathof et al., “Optical technologies for terabit/s-throughput feeder link,” in International Conference on Space Optical Systems, 2017.

[6] K. Broekens et al., “Adaptive Optics pre-correction Demonstrator for Terabit Optical Communication”, International Conference on Space Optics 2022.

[7] F. Silvestri et al., “High-Power Free-Space Bulk Multiplexer for Satellite Communication Optical Ground Terminal”, International Conference on Space Optics 2022.

[8] D. Sprung, P. Grossmann, E. Sucher, K. Weiss-Wrana en K. Stein, „Stability and height dependant variations of the structure function parameters in the lower atmospheric boundary layer investigated from measurements of the long-term experiment VERTURM (vertical turbulence measurements),” *Proceedings of SPIE Vo. 8178: Optics in Atmospheric Propagation and Adaptive Systems XIV ,* 2011.

[9] M. Pierzyna et al., “A multi-physics ensemble modeling framework for reliable estimation”, SPIE Proc. Environmental Effects on Light Propagation and Adaptive Systems VI. 2023.

[10] A Montmerle-Bonnefois et al., “Feasibility demonstration of AO pre-compensation for GEO feeder links in a relevant environment”, Optics Express Vol. 30, No. 26, 19 Dec 2022.

[11] K. Kudielka et al., “Successful first optical feeder link demonstration between a ground station and a GEO satellite applying adaptive optics pre-compensation”, Communications and Observations through Atmospheric Turbulence conference, Durham, March 2023.

[12] R. Sasiela and J. Shelton,”Guide star system considerations”, Chapter 3 in Adaptive Optics Engineering Handbook, 1st edition, CRC Press, 1999.